

Dynamic Covalent Dextran Hydrogels as Injectable, Self-adjuvating Peptide Vaccine Depots

Bowen Fan^{1,#}, Diana Torres García^{2,#}, Marziye Salehi^{1,2}, Sander I. van Kasteren^{2,*}, Rienk Eelkema^{1,*}

¹ Department of Chemical Engineering, Delft University of Technology
Van der Maasweg 9, 2629 HZ Delft, The Netherlands

² Leiden Institute of Chemistry and Institute of Chemical Immunology, Division of Bio-Organic Synthesis, Leiden University, Gorlaeus Laboratory, Einsteinweg 55, 2333 CC, Leiden, The Netherlands

equal contributions

* corresponding authors; e-mail: r.eelkema@tudelft.nl, s.i.van.kasteren@chem.leidenuniv.nl

Keywords: dynamic covalent hydrogels, vaccines, injectable gel, dextran, peptide antigens.

Abstract

Dextran-based hydrogels are promising therapeutic materials for drug delivery, tissue regeneration devices, and cell therapy vectors, due to their high biocompatibility, along with their ability to protect and release active therapeutic agents. This report describes the synthesis, characterization and application of a new dynamic covalent dextran hydrogel as an injectable depot for peptide vaccines. Dynamic covalent crosslinks based on double Michael addition of thiols to alkynones impart the dextran hydrogel with shear-thinning and self-healing capabilities, enabling hydrogel injection. These injectable, non-toxic hydrogels show adjuvant potential and have predictable sub-millimolar loading and release of the peptide antigen SIINFEKL, which after its release is able to activate T-cells, demonstrating that the hydrogels deliver peptides without modifying their immunogenicity. This work demonstrates the potential of dynamic covalent dextran hydrogels as a sustained-release material for delivery of peptide vaccines.

The success of vaccines is strongly dependent on the kinetics of antigen exposure and the subsequent cellular and humoral immune responses induced.^[1] Sustained antigenic exposure within tightly controlled release conditions is therefore sought after to prompt a durable and protective immune response.^[1-3] Sustained-release technologies such as nanoparticles, cationic lipids/liposomes, polysaccharides, and poly (lactic-co-glycolic acid) (PLGA) particles can provide these essential spatial and temporal interactions.^[3-5] Nevertheless, these systems must overcome some challenges such as tedious synthesis procedures, low drug loading capacity, or inability to deliver cargo. As for the cargo, the loaded antigens could face degradation and immunogenicity loss induced by changes in pH, temperature, oxidation/reduction reactions, or other chemical modifications.^[6] Thus, there is an urgent need for delivery systems capable of releasing unmodified antigens. In this regard, an excellent alternative for such systems can be found in hydrogels, as they can possess high biocompatibility as well as high loading capacity.^[7,8] Their hydrophilic nature enables the absorption of large amounts of fluid and bioactive cargo.

The use of hydrophilic polymer scaffolds ensures a low cellular and protein adherence to the gel interface, making them biocompatible.^[6,9] Viscoelastic properties and *in vivo* degradation characteristics can be tuned through molecular design.^[10,11] The chemical and mechanical properties of hydrogels determine the release kinetics of the cargo, which can be controlled by altering the polymer structure, the density, and type of crosslinker forming the hydrogel, as well as its degradation kinetics.^[12-14] Hydrogels can act as depots for the sustained release of antigens.^[15-17] These depot gels can be introduced in the body by grafting to the skin, surgical implantation, and through injection. Injection requires shear-thinning and self-healing properties that are not observed for permanently crosslinked polymer hydrogels but can be introduced through the use of reversible crosslinks. In this context, Appel et al. described a cellulose-derived hydrogel containing hydrophobic non-covalent crosslinks, for the sustained release of model protein antigens.^[15]

In an effort to develop injectable hydrogel antigen depots that do not use hydrophobic interactions, we were interested to evaluate the use of dextran polymers crosslinked through dynamic covalent bonds, for the release of peptide antigens. Peptide vaccines have been at the forefront in the recent spate of ‘molecularly defined’ anti-cancer vaccines.^[18,19] However, to date they have precluded hydrogel-based delivery; with only large protein antigens having been

delivered in injectable hydrogels. The small size and poor solubility of many antigenic peptides mean that delivering these agents presents additional restraints on the carrier materials.

Here we report the synthesis, characterization, and mechanical properties of an injectable dextran hydrogel containing dynamic covalent crosslinks, and evaluation of prolonged T-cell activation by the release of peptide antigens. The biocompatibility of dextran has been previously reported making this polymeric hydrogel a very suitable system for the controlled release of antigens.^[20–22] As a dynamic covalent crosslink, we use the double Michael addition of thiols to alkynes, affording a reversible dithiane link that will slowly degrade in the presence of small-molecule thiols. We demonstrate the feasibility of this novel dextran hydrogel as a delivery system, by loading it with the SIINFEKL peptide, a minimal CD8-restricted T-cell epitope peptide. Moreover, this peptide was successfully released without losing its immunogenicity and it was taken up and processed by dendritic cells, resulting in its efficient presentation in the context of MHC class I molecules, and the subsequent antigen-specific T-cell activation.

We have recently reported a polymer hydrogel that is crosslinked through thiol-alkyne Michael addition dynamic covalent chemistry.^[23] The gels were made from tetra-thiol PEG star polymers that react with a small molecule alkyne to form a β -dithiane carbonyl dynamic crosslink.^[24–26] Resulting from the presence of this dynamic covalent crosslink, these polymer gels are shear thinning and self-heal after a stress is removed. Because of that property, the gels can be injected using a syringe, where they form stable gel particles immediately upon exiting the needle. Combining injectability with high water content and crosslinks that show dynamic behavior under physiological conditions make these materials interesting candidates for evaluation as injectable antigen depot vehicles for vaccination.

The original research employed a tetrathiol PEG star polymer as the polymer backbone of the gel. Such star polymers have limited availability and are difficult to functionalize further. Moreover, the free thiol groups may form disulfides through oxidation, leading to undesired crosslinking. Building on this work, we opted to develop a dextran-based polymer with side chain grafted lipoic acid as a masked dithiol. Reduction of the lipoic acid disulfide leads to the formation of two thiol functionalities, which mostly revert to the ring closed disulfide upon oxidation, thereby avoiding undesired crosslinking. Using a graft copolymer instead of an end-functionalized star polymer allows control over the crosslink-to-polymer ratio. After reduction, the free thiols on the lipoic acid-functionalized dextran **P** can react with alkyne **A** to form a

polymer network crosslinked with dynamic covalent double Michael addition products (Figure 1).

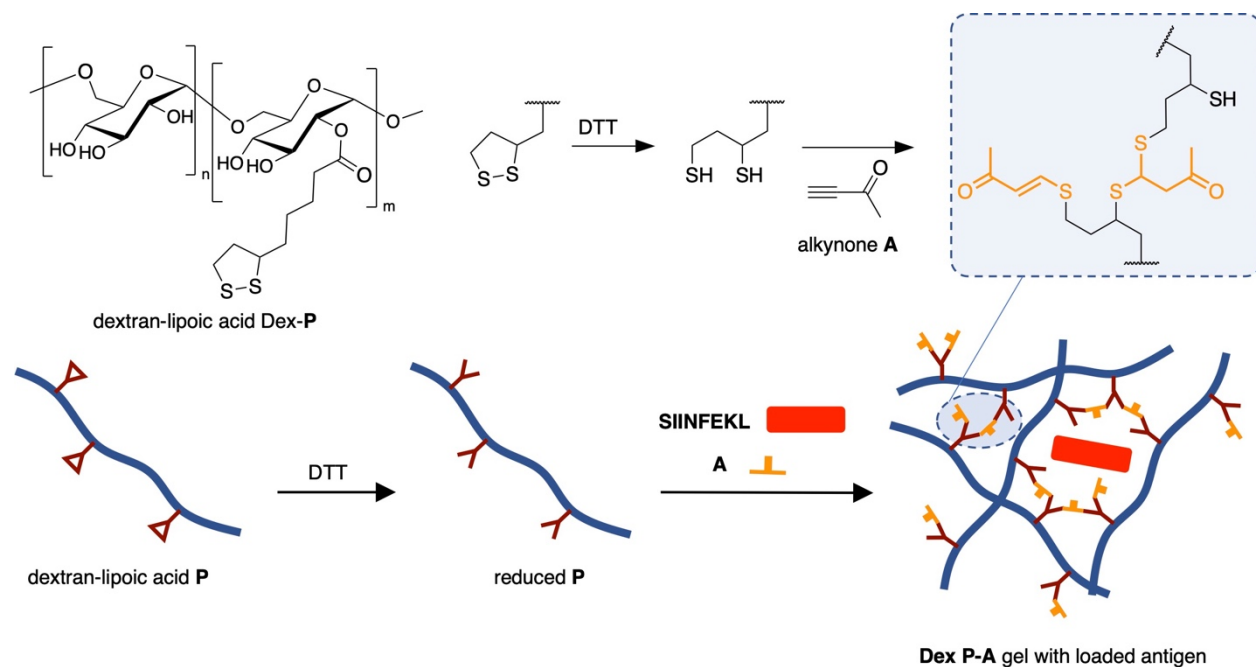


Figure 1. General concept and materials. Thiols formed by reduction of lipoic acid side chains on dextran polymer Dex-**P** react with alkyne **A**, to form the single and double Michael adducts. **A**-crosslinked polymer gels (Dex **P-A**) can be loaded with peptide antigens such as SIINFEKL and used for T-cell activation.

To make the hydrogel-vaccine, we first synthesized lipoic acid-functionalized dextran (Dex-**P**_x-**y**, with *x* indicating the dextran molecular weight, and *y* indicating the degree of functionalization with lipoic acid). We synthesized several versions of Dex-**P** using two methods: dextran was either reacted with lipoic acid anhydride catalyzed by dimethylaminopyridine (DMAP), or with lipoic acid catalyzed by DPTS (the 4-toluenesulfonate salt of DMAP). Starting from dextran with Mw=20 kDa, 70 kDa, and 500 kDa, we synthesized Dex-**P** polymers with degrees of substitution between 3.1 and 10.5 (Table 1). Dex-**P** polymers with a high degree of substitution were not sufficiently soluble in aqueous solvent, and were not investigated further. We next determined whether the polymers could form gels upon reaction with alkyne **A** in sodium phosphate buffer (100 mM phosphate, pH=8.2, “PB8.2”). For the dithiothreitol (DTT)-mediated reduction of native lipoic acid, we determined that around 67% disulfide is reduced in 10 minutes, using 1 eq. DTT in PB8.2 (Figure S6). Based on this result, we treated a polymer solution for 10 min.

with DTT (1 eq. with respect to the dithiolane ring content of the polymer) to reduce the lipoic acid sidechain disulfides. After DTT reduction, we added **A** (1 eq. to DTT), and the mixtures were left to react for 4 hours at room temperature to allow crosslink formation. Of the soluble Dex-**P** polymers, only the 70kDa dextran with DS=4.2 (**P70-4.2**), made using the anhydride method, showed gelation. This polymer formed a turbid hydrogel after activation with DTT and subsequent reaction with **A** (10 wt% polymer in PB8.2) (Figure 2a). **P70-4.2-d** synthesized by the DPTS catalysis method does not form a gel. This effect may be caused by different substitution patterns of dextran depending on the use of the anhydride method or DPTS. For **P70-4.2**, the ¹H NMR spectrum shows that lipoic acid esterification takes place mostly at the C2 hydroxyls of dextran (Figure S2). For **P70-4.2-d**, however, a new peak at 5.27 ppm in the ¹H NMR spectrum suggests substantial esterification at both C3 and C2 hydroxyls (Figure S5).^[27] All other polymers gave liquid solutions after incubation with **A**. The solubility and gelation results suggest that there is a fine balance between having enough lipoic acid groups per polymer chain to allow sufficient crosslink formation and having too many hydrophobic lipoic acid groups hindering solubility.

We investigated the process of hydrogel formation and the mechanical properties of the formed gels by rheological measurements. After reacting for 10 minutes with DTT, we added **A** to the solution of activated **P70-4.2**, and the mixture was transferred on the rheometer. A rheological time sweep shows a fast gelation, indicated by the crossover of storage modulus (G') and loss modulus (G'') after 5 minutes. After 6 h of reaction, G' approached an equilibrium value ($G' = 5.0$ Pa and $\tan \delta (G''/G') = 0.34$) (Figure S7a). A frequency sweep demonstrated that the hydrogel maintains a solid-like state in the range of 100 to 0.01 rad s⁻¹ (Figure 2b).

Table 1. Synthesis, solubility, and gelation of Dex-**P** with varying molecular weight and degree of substitution.

Dex- P	dextran Mw (kDa)	molar ratio of LA to AHG ^a	degree of substitution ^b	P solubility ^c	gelation ^e
P20-6.4	20	0.5	6.4	soluble	liquid ^d
P70-3.1	70	0.3	3.1	soluble	liquid ^d
P70-4.2	70	0.5	4.2	soluble	gel
P70-5.9	70	0.8	5.9	low solubility	-

P70-4.2-d ^f	70	0.4	4.2	soluble	liquid ^d
P70-6.8-d ^f	70	0.6	6.8	low solubility	-
P70-10.5-d ^f	70	0.7	10.5	low solubility	-
P500-4.8	500	0.5	4.8	low solubility	-

^a Molar feeding ratio of lipoic acid or lipoic acid anhydride to AHG of dextran during the synthesis of Dex **P-A**. ^b Degree of substitution is defined as the number of attached lipoic acid units per 100 AHG units of dextran and calculated by ¹H NMR according to the protons of the attached lipoic acid group at 3.10 ppm and the dextran glucosidic protons at 4.85 and 5.19 ppm. ^c In PB8.2 (20 mg in 180 μ L buffer). Low solubility means that even stirred overnight or processed with ultra-sonication for 1 h does not lead to complete solubilization. ^d The sample still shows flow after 1 day reaction time, checked by the vial-inversion method. ^e Hydrogel formation (10 wt% polymer in PB8.2) was checked by the vial-inversion method. Gel formation means the sample shows no flow within 1 minute after inversion. ^f Synthesized from dextran-70k and lipoic acid catalyzed by DPTS.

The critical strain (γ) needed to induce a gel-sol transition was determined by a strain sweep from 1 to 1200 % (Figure S7c), showing a crossover point of G' and G'' at around 1000%. We then examined the ability to self-heal by a continuous step-strain sweep using a cyclic 1% to 1200% strain program (Figure 2c). Upon applying a 1200% strain to the hydrogel, G'' becomes higher than G' , which means that the hydrogel turns to a fluid state. When the applied strain turned to 1%, G' recovered back immediately to around 3 Pa and $\tan \delta < 1$, suggesting a rapid self-healing of the hydrogel. At a second strain cycle, the hydrogel again showed self-healing after fluidization and G' again subsequently recovered to the initial value. In addition, we demonstrated the self-healing ability of the hydrogel by a macroscopic self-healing test (Figure 2e). Two cube-shaped Dex **P-A** hydrogels (4 \times 10 \times 10 mm) were colored yellow and red by fluorescein and rhodamine B dyes, respectively. The two hydrogels were then weakly pressed together and kept in a humid atmosphere to allow self-healing. After 10 minutes, the two hydrogels had connected and the resulting gel could be lifted using a tweezer, without the newly formed connection failing. The crack between the two gels subsequently disappeared, enabling observable diffusion of dyes across the interface (Figure 2d). We demonstrated injection of the

hydrogel by extruding a colored Dex **P-A** hydrogel through a 20G syringe needle (Figure 2e). After exiting the needle, the gel healed immediately and could be drawn as an ink.

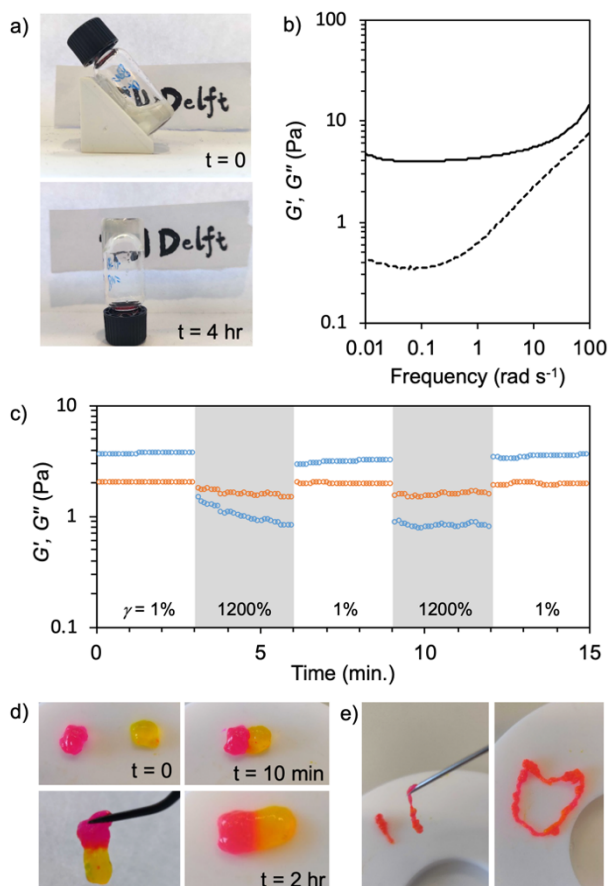


Figure 2. Dex **P-A** hydrogel formation and its mechanical properties, self-healing, and injectability. a) Hydrogel formation by mixing **P70-4.2**, DTT, and alkyne **A** PB8.2 solutions sequentially: after 10 minutes of mixing **P70-4.2** and DTT solutions, **A** in PB8.2 was added into the mixture, initiating the gelling process (top); after 4 h reaction, a slightly turbid hydrogel formed, that could hold its own weight when inverted (bottom). b) Rheological frequency sweep of the hydrogel 6 h after mixing, showing that G' (solid line) is higher than G'' (dashed line) over the entire frequency range (strain (γ) = 0.5%, frequency = 100-0.01 rad s^{-1} , 25 °C). c) Continuous step strain measurement of the hydrogel, strain is switched from 1% to 1200% for two cycles. d) Macroscopic self-healing of the hydrogel. Two cube-shaped gels (4x10x10 mm) were colored red and yellow using rhodamine B and fluorescein, respectively (top left). The two gels were pressed together and found to have connected after 10 min (top right). The rejoined gel can be lifted using a tweezer (bottom left). After 2 h, the interface between the two gels had disappeared

and the dyes could diffuse over the interface (zoom, bottom right). e) A 0.6 ± 0.2 mm strip-shaped hydrogel formed after hand-pressed extrusion through a 20G syringe needle (left). Rhodamine B was added to the gels for visualization. The extruded structures could hold their shape over extended periods (right).

We next determined the cytotoxicity of the Dex **P-A** hydrogel to immune cells. For this, the dendritic cell line D1^[28] was cultured on Dex **P-A** hydrogel and the viability was evaluated through an MTT assay. This assay measures the reduction of MTT into formazan by mitochondrial succinate dehydrogenase.^[29] The concentration of formazan is directly proportional to the number of live cells; therefore, possible detrimental intracellular effects on metabolic activity associated with hydrogel toxicity will influence the outcome. The D1 cells were cultured on Dex **P-A** for 24 and 48 h prior to washing off the hydrogel with PBS to remove excess free reagent and any soluble by-product. Under these conditions, $82 \pm 11\%$ and $79 \pm 9\%$ of D1 cells survived after 24 h and 48h of incubation, respectively (Figure 3). If the washing step was omitted, viability decreased by approximately 30% ($p < 0.05$ compared with 24 and 48 h incubation times), suggesting residual soluble components of the gel formation being toxic to the cells.

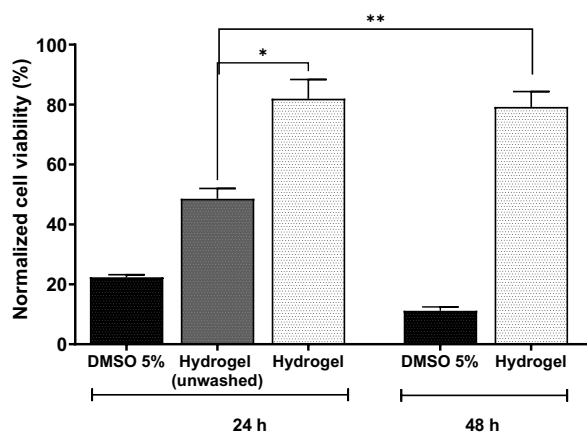


Figure 3. Cell viability on the Dex **P-A** hydrogel. MTT assay in D1 cells cultured on Dex **P-A** hydrogel incubated for 24 and 48 h at 37°C, 5% CO₂, and 95% humidity. Error bars represent the standard error of the mean. Data correspond to 3 independent experiments. The asterisks indicate the difference between the unwashed Dex **P-A** hydrogel and the other hydrogels. * $p = 0.01$ ** $p = 0.007$.

To assess the potential of these hydrogels as a peptide vaccine delivery systems, we evaluated the release of the commonly used minimal CD8-restricted T-cell epitope peptide SIINFEKL^[30] from the Dex **P-A** hydrogel. For this, Dex **P-A** hydrogels were loaded with three different concentrations of SIINFEKL (1, 10, and 100 μ M). The release of SIINFEKL over time was detected through an (*in vitro*) T-cell activation assay, where the amount of peptide is quantified using the T-cell clone B3Z that carries a LacZ gene under the NFAT promoter, that allows it to produce beta-galactosidase in response to the peptide loaded on MHC-I in a concentration dependent manner.^[31] This in turn can be quantified using the conversion of the luminogenic substrate chlorophenol red- β -D-galactopyranoside (CPRG). Figure 4 shows that the release rate of the SIINFEKL from the Dex **P-A** hydrogels is influenced by the concentration of peptide loaded in the hydrogels. In this regard, the maximum cumulative % of SIINFEKL release at 48 hours is 15, 27, and 37 % for the Dex **P-A** hydrogels loaded with 1, 10, and 100 μ M of SIINFEKL, respectively (Figure 4a-c). An experiment at the higher 1000 μ M concentration (Figure S8) confirmed this trend.

Based on the above, we compared the release profiles of SIINFEKL at 48 h from Dex **P-A** hydrogels loaded with 1, 10, 100, and 1000 μ M concentrations (Figure 4d). The total amount of SIINFEKL released is related to the loading concentration by a power law with a 0.23 exponent. Combined, these results suggest that the loaded peptide is entrapped within the mesh network of the Dex **P-A** hydrogel and released either as degradation of the hydrogel matrix occurs, or through diffusion from the intact matrix. The time-dependent release data (Figure 4 a-c) does not show zeroth or first order kinetics, and has only a partial fit to the Higuchi equation^[32], suggesting that release is not merely governed by Fickian diffusion from the hydrogel matrix. A time lag observed in all release profiles also suggests that changes to the hydrogel network play a role in the release. A fit to the Korsmeyer-Peppas model^[33] shows that, after the lag time, the release process is initially largely dominated by Fickian diffusion (exponent $n \sim 0.5$) followed by an increase of n on longer time scales, suggesting a combination of diffusion and hydrogel erosion. We therefore postulate that both diffusion and degradation play a role in the release, with relative contributions changing over time. Interestingly, only the gel with the extreme 1000 μ M loading showed a burst release. No burst phase release of the peptide antigen was observed at the more relevant 1-100 μ M loading concentrations.

The cumulative percentage of SIINFEKL release at 48 h indicates that significant amounts of SIINFEKL are retained in the hydrogel. We therefore measured the residual T-cell activation capacity of the 48h gels. For this purpose, we disrupted the remaining hydrogel mechanically, and incubated the residue at 37 °C for 20 minutes. After this time, the gel had dissolved completely, confirming its biodegradation potential. We subsequently pulsed D1 cells with the dissolved gels and measured T-cell activation. Interestingly, the Dex **P-A** hydrogel by itself was also able to activate the B3Z T-cells. This result suggests that the Dex **P-A** hydrogel in itself has immunostimulatory properties. This could be beneficial for increasing antigen-presenting cell (APC) activation, as has been reported in previous studies with other hydrogels and protein-dextran conjugates.^[2,34] This T-cell activation induced by non-loaded hydrogels (Figure S8) hints towards a potential local inflammatory niche formation capacity, that could enhance immune responses. However, the impact of their specific niche properties, its persistence, and relevance to the immune response induced must be explored in future *in vivo* assays.

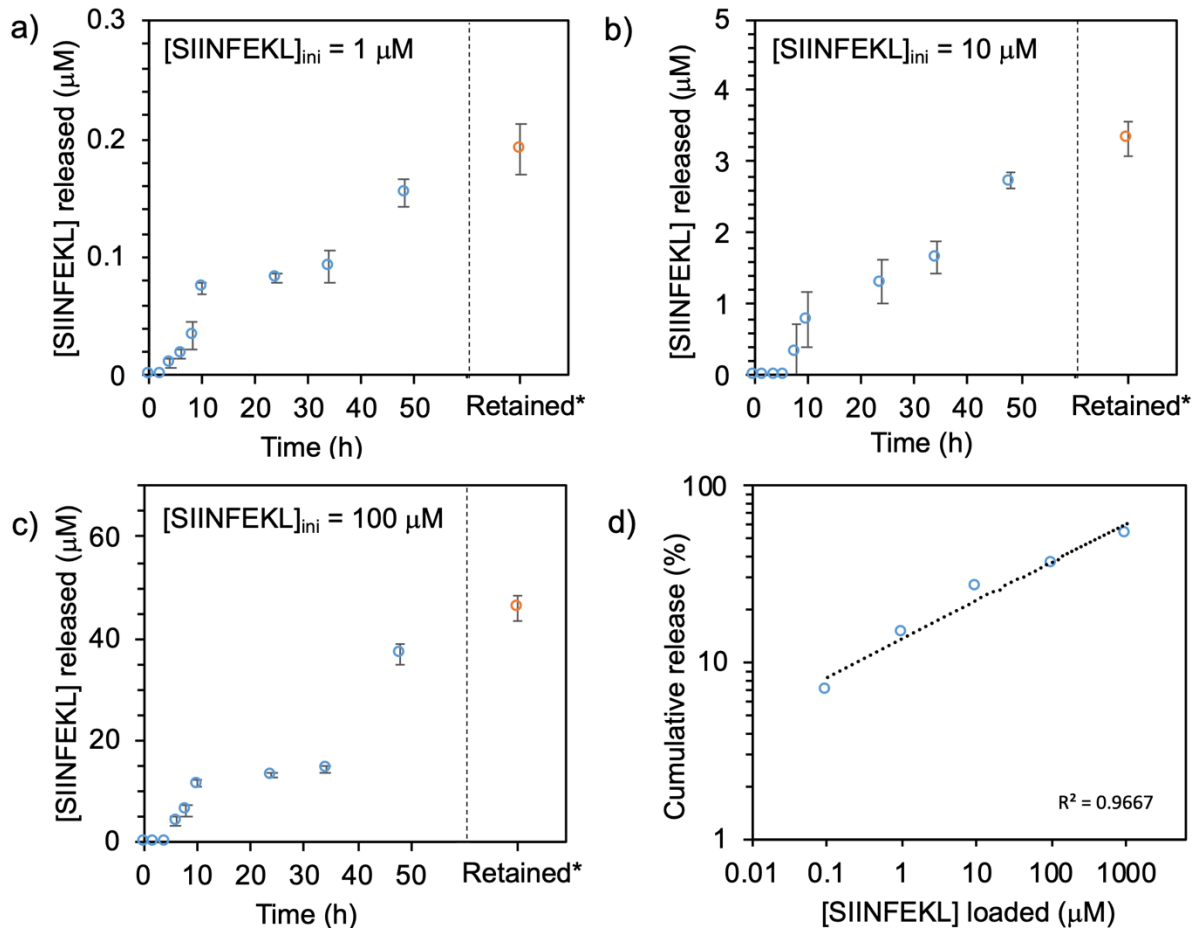


Figure 4. SIINFEBKL release from the hydrogel. SIINFEBKL release from Dex **P-A** hydrogel over a 48 h period. D1 cells were pulsed for 3 h with supernatant released from Dex **P-A** hydrogel loaded with 1 μM (a), 10 μM (b), 100 μM (c) of SIINFEBKL, and then co-cultured with B3Z cells to analyze their activation. *Retained indicates SIINFEBKL retained in the remaining hydrogel after 48 h. d) SIINFEBKL release profile at 48 h of Dex **P-A** hydrogels loaded with 1, 10, 100 and 1000 μM concentrations, plotted on a double logarithmic scale. The data fits a power law with a 0.23 ± 0.02 slope, describing the relation between loaded and released peptide. Error bars represent the SD. Data correspond to 4 independent experiments (n=2 replicates per experiment).

In this work, we show how dextran derived polymer gels can act as injectable depots for sustained release of vaccines. We developed a dextran polymer that is crosslinked using a dynamic covalent double Michael addition of thiols to alkynes. Using a masked thiol prevents undesired oxidative thiol crosslinking of the matrix polymer. The obtained hydrogels are shear thinning and self-healing, and can be injected through a 20G needle, forming stable gel particles immediately after extrusion. These hydrogels show acceptable viability of dendritic cells, suggesting that they are compatible for interacting with the immune system. *In vitro* tests show slow, sustained release of loaded SIINFEBKL minimal epitope, as measured by T-cell activation essays. The rate of T-cell activation depends on the concentration of loaded antigen. This, combined with the observed self-adjuvating properties of the hydrogels, suggest that they could find application as injectable depots for slow and prolonged release of vaccines, which could be used to achieve augmented vaccination response.

Experimental Section

NMR spectra were recorded on an Agilent-400 MR DD2 (399.7 MHz for ^1H and 100.5 MHz for ^{13}C) at 298 K. The rheological measurements were performed using a rheometer (AR G2, TA instruments) equipped with a steel plate-and-plate geometry of 40 mm in diameter and equipped with a hexadecane trap. Dithiothreitol, lipoic acid (LA) and 3-butyn-2-one were purchased from Fluorochem ltd. Dextran-500k ($M_n = 500$ kDa) and dextran-20k ($M_n = 20$ kDa) were purchased from Alfa Aesar. Dextran-70k ($M_n = 70$ kDa), N,N'-dicyclohexylcarbodiimide (DCC), p-

toluenesulfonic acid monohydrate and 4-(dimethylamino) pyridine (DMAP) were purchased from Sigma Aldrich. 4-(Dimethylamino)pyridinium 4-toluenesulfonate (DPTS) was synthesized according to previous literature.^[35] The technical solvents were purchased from VWR and the reagent grade solvents were purchased from Sigma Aldrich.

Cell lines and culture: D1 and B3Z (OVA₂₅₇₋₂₆₄-specific, H2kb-restricted CTL hybridome) cell lines were cultured in IMDM (Iscove's Modified Dulbecco's Medium) complete medium, supplemented with 10% heated-inactivated fetal calf serum (FCS), antibiotics (100 µg mL⁻¹ streptomycin and 100 IU mL⁻¹ penicilin), 2 mM glutamine (glutamax), and 50 mM 2-β mercaptoethanol. In addition, the D1 cell-medium was supplemented with 30% rGM-CSF mouse (10-20 ng mL⁻¹). This growth factor was collected and filtered from the supernatant of NIH/3T3 cell-cultures. The cell lines were cultured at 37°C with 95% relative humidity and 5% CO₂ atmosphere. Cultured cells were harvested by PBS-EDTA and washed two times with medium.

Synthesis of Lipoic acid anhydride: Lipoid acid anhydride was synthesized based on the method described by previous literature.^[36] A mixture of lipoic acid (6.00 g, 29.08 mmol) and DCC (3.60 g, 17.45 mmol) was stirred in 80 mL of anhydrous dichloromethane at room temperature under nitrogen atmosphere. After 20 hours, the product mixture was filtered to remove dicyclohexylurea and solvent was removed by rotary evaporation. The product was dried in an oven overnight to obtain a yellow solid (3.59 g, yield: 60 %). The product was directly used in next step without purification.

Synthesis of lipoic acid-functionalized dextran P1 by esterification with acid anhydride method: Lipoic acid-functionalized dextran (Dex-P) was synthesized based on the method described in the literature.^[37] Dextran-70k (1.41 g, containing 8.69 mmol AHG), 4-(dimethylamino) pyridine (1.06 g, 8.69 mmol) and lipoic acid anhydride (1.72 g, 4.35 mmol, ratio of lipoic acid anhydride to anhydroglucosidic rings of dextran (AHG) is 0.5) were dissolved to 20 mL anhydrous DMSO. The mixture was stirred for 48 hours at 50 °C. Then, the product was precipitated in cold ethanol. The precipitation was collected by centrifugation and dissolved in water. The mixture solution was transferred to a dialysis bag (MWCO = 14kDa) and dialyzed by distilled water for 2 days. The white solid was obtained after freeze-drying (“P70”, 0.47 g, yield, 34%). The degree of substitution (DS, defined as the number of attached lipoic acid rings per 100 AHG unit) is 4.2 determined by ¹H NMR (ratio based on the integration of peak at 3.10 ppm and the integration of peaks at 4.85 and 5.19). ¹H NMR (399.7 MHz, D₂O) δ 5.19, 5.05,

4.85 (m, dextran anomeric protons), 3.62 (m, hydroxyl of dextran), 3.10 (m, -SS-CH₂-CH₂-CH), 2.37 (m, -SS-CH₂-CH₂-CH and -CH₂-COO), 1.88 (m, -SS-CH₂-CH₂-CH), 1.63, 1.54, 1.35 (m, -CH₂-CH₂-CH₂-dithiolane ring).

Dex-**P** based on dextran-500k (**P500**) and Dex-**P** based on dextran-20k (**P20**) were synthesized by the same procedure as described above.

P70 with varying degree of substitution (3.1 and 5.9) were obtained by using different molar ratios of lipoic acid anhydrides to AHG of dextran (0.3 and 0.8).

Synthesis of lipoic acid-functionalized dextran P70d by esterification using DPTS as a catalyst system: Dextran-70k (0.981 g, containing 6.05 mmol AHG), lipoic acid (0.5 g, 2.42 mmol, 0.4 eq. to AHG of Dextran), DPTS (0.107 g, 0.363 mmol, 0.15 eq. to acid) and DCC (0.75 g, 7.27 mmol) were dissolved to 30 mL anhydrous DMSO. The mixture was stirred for 24 hours at room temperature. Then, undissolved *N,N'*-dicyclohexylurea was removed by filtration. The solution was precipitated in cold ethanol. The precipitation was collected by centrifugation and dissolved in water. The mixture solution was transferred to a dialysis bag (MWCO = 14kDa) and dialyzed against distilled water for 2 days. The white solid was obtained after freeze-dried ("**P70d**", 0.92 g, yield, 94%).

P70d with varying degree of substitution (6.8 and 10.5) were obtained by using different molar ratios of lipoic acid anhydrides to AHG of dextran (0.6 and 0.7).

Reduction Model reaction: The aim of the small molecule model reaction is to study the reduction of the lipoic acid dithiolane ring by DTT in PB8.2. The reaction of sodium lipoate and DTT was followed by ¹H NMR. To a solution of sodium lipoate (5 mg, 0.02 mmol) in PB8.2 (450 μL) and 4 drops of D₂O, a solution of DTT (3.4 mg, 0.02 mmol) in PB8.2 (500 μL) was added and the reaction was checked after 10 minutes by ¹H NMR at room temperature.

Preparation of Dex P-A hydrogels: **P70-4.2** (40 mg, containing 0.0104 mmol lipoic acid group) was dissolved in 360 μL phosphate buffer solution (100 mM, pH=8.2; 'PB8.2'). The mixture was stirred for 15 minutes at room temperature to dissolve Dex-**P** completely. Dithiothreitol (16 mg, 0.104 mmol, "DTT") was dissolved in 200 μL PB8.2 as DTT pre-solution. 3-Butyn-2-one **A** (8.2 μL, 0.104 mmol) was added in 200 μL PB8.2 as alkynone **A** pre-solution. 20 μL DTT pre-solution (0.0104 mmol) was added to the Dex-**P** solution and stirred for 10 minutes. Then 20 μL **A** pre-solution (0.0104 mmol) was added. A turbid hydrogel (40 mg

polymer in 400 μL , 10 wt%) formed after 4 hours in a 1.5 mL glass vial at room temperature. Gelation was checked by the vial inversion method every half an hour.

P70 with varying DS (3.1 and 5.9), **P500-4.8**, **P20-6.4** and **P70d** with varying DS (4.2, 6.8 and 10.5) were tested for gelation by the method described above.

Rheological measurements of hydrogels: A Dex **P-A** hydrogel was prepared as described above. A 500 μL solution of pre-gel solution was positioned on the rheometer plate. Time sweep measurements were performed at fix strain ($\gamma = 0.5\%$) and frequency ($\omega = 6.28 \text{ rad/s} = 1 \text{ Hz}$). Frequency sweep measurements were performed from 100 to 0.01 rad/s at fix strain ($\gamma = 0.5 \%$). All frequency sweeps were measured after storage modulus (G') reached equilibrium state. All measurements were performed in the linear viscoelastic region. The modulus of hydrogels was measured under strain sweep from 1 to 1200% at a fixed frequency ($\omega = 6.28 \text{ rad/s}$). Continuous step strain measurements were measured at fixed frequency ($\omega = 6.28 \text{ rad/s}$). Oscillatory strains were switched from 1% strain to subsequent 1200% strain with 3 minutes for every strain period.

Self-healing test and injection of hydrogel: Two pieces of cube-shaped hydrogel ($4 \times 10 \times 10 \text{ mm}$) were prepared as described above colored by rhodamine B (red dye) and fluorescein (yellow dye). Then two piece of different color hydrogels were brought together and kept in a moist environment for 10 minutes. Afterwards, this healed hydrogel was cut to 4 equal pieces using a scalpel. Then a piece of hydrogels was put in a syringe (1 mL volume; 0.5 inner diameter) using a tweezer and syringe plunger, and subsequently injected through a 20G needle using manual force.

Cell viability assay: The cytotoxicity of the Dex **P-A** hydrogel was evaluated through an MTT (tetrazolium (3-(4,5-dimethylthiazol-2-yl)-2,5-diphenyltetrazolium bromide) assay, as previously described.^[29] Briefly, 85 μL of Dex **P-A** hydrogel were added per well to a 96-well tissue-culture plate. The hydrogel was washed by adding 100 μL of PBS to eluted unreacted reagents. Then, D1 cells (100 000 cells per well) were added in 150 μL of IMDM complete medium. As a negative control of toxicity, D1 cells on IMDM complete medium were used. In addition, DMSO (5%) was used as a positive control of toxicity. The cells were incubated with the Dex **P-A** hydrogel for 24 or 48 h at 37°C, 5% CO_2 , and 95% humidity. Next, cells were spun down three minutes at 300xg at room temperature. Later, the medium was removed from each well and replaced with 90 μL of IMDM complete medium. Then 10 μL of MTT (final concentration of 0.5 mg/ml in PBS) was added to each well and incubated for 3 h at 37°C, 5%

CO₂, and 95% humidity. The formazan was precipitated by centrifugation, the medium was removed, and 100 µL of DMSO was added to each well to dissolve the formazan crystals. The plate was incubated for 30 min at 37°C, with 5% CO₂, and 95% humidity. Absorbance at 570 nm was measured using a CLARIOstar plate reader. The number of surviving cells is directly proportional to the amount of formazan product. Results were normalized between untreated cells as 100% and only media as background signal.

SIINFEKL release assay: To evaluate indirectly the release of SIINFEKL from the Dex **P-A** hydrogel a T-cell activation assay was carried out as previously described.^[31] Briefly, 1, 10, and 100 µM of SIINFEKL peptide were added to Dex **P-A** hydrogel. Then 85 µL of hydrogel was added per well to a 96-well tissue-culture plate. The hydrogel was washed with 100 µL of PBS 1x and later incubated with 100 µL of fresh IMDM medium for 2, 4, 6, 8, 10, 24, 34, and 48 h at 37°C, 5% CO₂, and 95% humidity. The supernatant removed from the Dex **P-A** hydrogel was diluted 1:100, 1:1000 and 1:10000 for the 1, 10, and 100 µM of SIINFEKL loaded hydrogel, respectively. The D1 cells (50 000 cells/well) were seeded in a 96-well plate and allowed to adhere to the plate for 1 h at 37°C, 5% CO₂, and 95% humidity. The diluted supernatant was added to the D1 cells. The D1 cells were pulsed with 100 µL of each supernatant timeslot for 3h at 37°C, 5% CO₂, and 95% humidity. The cells were spin down at 300xg per 5 min, the medium was removed, and 50 000 B3Z T-cells were added per well. Co-cultures were incubated overnight (15h) at 37°C, 5% CO₂, and 95% humidity.

The T-cell activation was measured as beta-galactosidase-directed CPRG (chlorophenol red-β-galactopyranoside) hydrolysis. The B3Z T-cell line carries a lacZ construct driven by NFAT, therefore the CPRG assay has a direct correlation with IL-2 promotor activity. For the CPRG assay, 100 µL of lysis buffer were added per well and incubated for 4 h at 37°C in the dark. The absorbance was measured at 570 nm in a CLARIOstar plate reader.

For each assay, a standard curve was performed to interpolate the concentration of SIINFEKL available to pulsed dendritic cells and therefore activated the B3Z cells. In this regard, the data was interpolated into a curve of 5-0.1 nM of SIINFEKL peptide using a lineal regression.

Statistical analysis: Mean and Standard Error of Mean (SEM) and Standard Deviation (SD) were calculated for each variable studied. Based on the normality test, the difference between groups were assessed using a parametric test (t test). To interpolate the standard curve, we used a logarithmic regression. In all cases, a value of p<0.05 was considered statistically significant. All

graphics were performed using GraphPad Prism software, version 6.00 for MAC (GraphPad Software, La Jolla, California, USA, www.graphpad.com), and the statistical analyses was performed in R Studio (Version 0.98.1091 - © 2009–2014 RStudio, Inc.) using the package *pracma*.

Acknowledgements

Financial support by the Chinese Scholarship Council (B.F.) and the European Research Council (R.E., ERC consolidator grant 726381) is acknowledged.

Conflict of Interest

The authors declare no financial/commercial conflict of interest.

References

- [1] D. J. Irvine, M. A. Swartz, G. L. Szeto, *Nat. Mater.* **2013**, *12*, 978.
- [2] A. Lees, F. Finkelman, J. K. Inman, K. Witherspoon, P. Johnson, J. Kennedy, J. J. Mond, *Vaccine* **1994**, *12*, 1160.
- [3] K. M. Cirelli, D. G. Carnathan, B. Nogal, J. T. Martin, O. L. Rodriguez, A. A. Upadhyay, C. A. Enemuo, E. H. Gebru, Y. Choe, F. Viviano, C. Nakao, M. G. Pauthner, S. Reiss, C. A. Cottrell, M. L. Smith, R. Bastidas, W. Gibson, A. N. Wolabaugh, M. B. Melo, B. Cossette, V. Kumar, N. B. Patel, T. Tokatlian, S. Menis, D. W. Kulp, D. R. Burton, B. Murrell, W. R. Schief, S. E. Bosinger, A. B. Ward, C. T. Watson, G. Silvestri, D. J. Irvine, S. Crotty, *Cell* **2019**, *177*, 1153.
- [4] A. Bolhassani, S. Safaiyan, S. Rafati, *Mol. Cancer* **2011**, *10*, 3.
- [5] D. T. O'Hagan, H. Jeffery, M. J. J. Roberts, J. P. McGee, S. S. Davis, *Vaccine* **1991**, *9*, 768.
- [6] N. A. Peppas, P. Bures, W. Leobandung, H. Ichikawa, *Eur. J. Pharm. Biopharm.* **2000**, *50*, 27.
- [7] S. Naahidi, M. Jafari, M. Logan, Y. Wang, Y. Yuan, H. Bae, B. Dixon, P. Chen, *Biotechnol. Adv.* **2017**, *35*, 530.
- [8] L. García-Fernández, M. Olmeda-Lozano, L. Benito-Garzón, A. Pérez-Caballer, J. San Román, B. Vázquez-Lasa, *Mater. Sci. Eng. C* **2020**, *110*, 110702.
- [9] T. Vermonden, R. Censi, W. E. Hennink, *Chem. Rev.* **2012**, *112*, 2853.
- [10] P. B. O'Donnell, J. W. McGinity, *Adv. Drug Deliv. Rev.* **1997**, *28*, 25.
- [11] P. Sansdrap, A. J. Moës, *Int. J. Pharm.* **1992**, *98*, 157.
- [12] S. Pacelli, P. Paolicelli, M. A. Casadei, *Carbohydr. Polym.* **2015**, *126*, 208.

- [13] W. E. Hennink, C. F. van Nostrum, *Adv. Drug Deliv. Rev.* **2002**, *54*, 13.
- [14] A. M. Kloxin, C. J. Kloxin, C. N. Bowman, K. S. Anseth, *Adv. Mater.* **2010**, *22*, 3484.
- [15] G. A. Roth, E. C. Gale, M. Alcántara-Hernández, W. Luo, E. Axpe, R. Verma, Q. Yin, A. C. Yu, H. Lopez Hernandez, C. L. Maikawa, A. A. A. Smith, M. M. Davis, B. Pulendran, J. Idoyaga, E. A. Appel, *ACS Cent. Sci.* **2020**, *6*, 1800.
- [16] S. D. Allison, *J. Pharm. Sci.* **2008**, *97*, 2022.
- [17] R. Langer, J. Folkman, *Nature* **1976**, *263*, 797.
- [18] C. J. M. Melief, T. van Hall, R. Arens, F. Ossendorp, S. H. van der Burg, *J. Clin. Invest.* **2015**, *125*, 3401.
- [19] P. A. Ott, Z. Hu, D. B. Keskin, S. A. Shukla, J. Sun, D. J. Bozym, W. Zhang, A. Luoma, A. Giobbie-Hurder, L. Peter, C. Chen, O. Olive, T. A. Carter, S. Li, D. J. Lieb, T. Eisenhaure, E. Gjini, J. Stevens, W. J. Lane, I. Javeri, K. Nellaiappan, A. M. Salazar, H. Daley, M. Seaman, E. I. Buchbinder, C. H. Yoon, M. Harden, N. Lennon, S. Gabriel, S. J. Rodig, D. H. Barouch, J. C. Aster, G. Getz, K. Wucherpfennig, D. Neuberg, J. Ritz, E. S. Lander, E. F. Fritsch, N. Hacohen, C. J. Wu, *Nature* **2017**, *547*, 217.
- [20] G. Sun, C. C. Chu, *Carbohydr. Polym.* **2006**, *65*, 273.
- [21] S. Mitra, U. Gaur, P. C. Ghosh, A. N. Maitra, *J. Control. Release* **2001**, *74*, 317.
- [22] S. R. Van Tomme, W. E. Hennink, *Expert Rev. Med. Devices* **2007**, *4*, 147.
- [23] B. Fan, K. Zhang, Q. Liu, R. Eelkema, *ACS Macro Lett.* **2020**, *9*, 776.
- [24] G. Joshi, E. V Anslyn, *Org. Lett.* **2012**, *14*, 4714.
- [25] H.-Y. Shiu, T.-C. Chan, C.-M. Ho, Y. Liu, M.-K. Wong, C.-M. Che, *Chem. Eur. J.* **2009**, *15*, 3839.
- [26] N. Van Herck, D. Maes, K. Unal, M. Guerre, J. M. Winne, F. E. Du Prez, *Angew. Chem. Int. Ed.* **2020**, *59*, 3609.
- [27] T. Liebert, S. Hornig, S. Hesse, T. Heinze, *J. Am. Chem. Soc.* **2005**, *127*, 10484.
- [28] C. Winzler, P. Rovere, M. Rescigno, F. Granucci, G. Penna, L. Adorini, V. S. Zimmermann, J. Davoust, P. Ricciardi-Castagnoli, *J. Exp. Med.* **1997**, *185*, 317.
- [29] M. B. Hansen, S. E. Nielsen, K. Berg, *J. Immunol. Methods* **1989**, *119*, 203.
- [30] O. Röttschke, K. Falk, S. Stevanović, G. Jung, P. Walden, H. G. Rammensee, *Eur. J. Immunol.* **1991**, *21*, 2891.
- [31] J. Karttunen, N. Shastri, *Proc. Natl. Acad. Sci. U. S. A.* **1991**, *88*, 3972.
- [32] J. Long, A. V Nand, C. Bunt, A. Seyfoddin, *Pharm. Dev. Technol.* **2019**, *24*, 839.
- [33] M. L. Bruschi, Ed. , in *Strategies to Modify Drug Release from Pharmaceutical Systems*, Woodhead Publishing, **2015**, pp. 63–86.
- [34] K. Adu-Berchie, D. J. Mooney, *Acc. Chem. Res.* **2020**, *53*, 1749.
- [35] J. S. Moore, S. I. Stupp, *Macromolecules* **1990**, *23*, 65.

- [36] A. Sadownik, J. Stefely, S. L. Regen, *J. Am. Chem. Soc.* **1986**, *108*, 7789.
- [37] Y.-L. Li, L. Zhu, Z. Liu, R. Cheng, F. Meng, J.-H. Cui, S.-J. Ji, Z. Zhong, *Angew. Chem. Int. Ed.* **2009**, *48*, 9914.